Inorganic Chemistry

Article

pubs.acs.org/IC

$Ba_3TM_2Se_9$ (TM = Nb, Ta): Synthesis and Characterization of New Polyselenides

Ming-Yan Chung and Chi-Shen Lee*

Department of Applied Chemistry, National Chiao Tung University, 1001 University Road, Hsinchu 30010, Taiwan

Supporting Information

ABSTRACT: New ternary polyselenides $Ba_3TM_2Se_9$ (TM = Nb, Ta) were synthesized through a solid-state reaction, and their structures were characterized using single-crystal X-ray diffraction. These compounds crystallized into a new structural type with a monoclinic space group $P2_1/c$. The structures were constructed from distorted, close-packed layers of $^3_\infty[BaSe_3]^{3.33-}$ that incorporated TM atoms at octahedral sites and contained $[(TM^{5+})_2(Se^{2-})_7(Se_2^{2-})]$ units. Diffuse reflectance spectra and electronic resistivity measurements indicated semiconducting properties and optical band gaps of 1.3 eV for $Ba_3Nb_2Se_9$ and 1.6 eV for $Ba_3Ta_2Se_9$. Raman spectra were used to investigate the interatomic interactions. Calculations of the electronic structure verified the semiconducting behavior and bonding interaction of short Se−Se contacts.

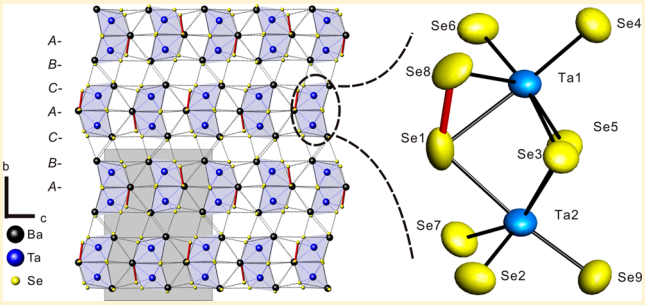

INTRODUCTION

Polychalcogenides are chalcogen-rich compounds that contain partially reduced chalcogen atoms with homonuclear chalcogen bonds in various shapes and lengths. These materials have received interest for decades because of their unique structural features and potential use in applications such as thermoelectric devices[1] and ion-exchange.[2] The homonuclear bonds of the polychalcogenides contained hypervalent interactions, which indicated the diversity of structures and coordination. Concerning polysulfides, the S_n^{2-} ($n > 1$) units exhibited 2c−2e bonds forming one-dimensional (1D) structures. For example, the binary polysulfides Rb_2S_2,[3] Rb_2S_3,[4] and Rb_2S_5[5] contained dumbbell, bent, and zigzag shaped anions, respectively. For polyselenides, interactions of the types 2c−2e and 3c−4e were observed in various 1D motifs of Se_n^{x-} (n = 2−6; x = 2, 4). Examples of the Se_3^{4-} unit with an approximately linear conformation and 3c−4e bonds were found in the crystal structures of $Rb_{12}Nb_6Se_{35}$[6] and $Ba_2Ag_4Se_5$.[7] In addition, building units of an infinity chain and a network of polyselenide were discovered in $La_2U_2Se_9$[8] and Cs_3Se_{22},[9] respectively. Polytellurides typically exhibit complex coordination modes because of their secondary coordination interactions between tellurium atoms. Te_n^{x-} units, including V-shaped $^1_\infty[Te_4^{4-}]$ and planar $^2_\infty[Te_6^{3-}]$ moieties, are found in the crystal structures of $CsCe_3Te_8$[10] and Cs_3Te_{22},[11] respectively.

Multinary polychalcogenides typically contain one or more electropositive elements, which might include alkali, alkaline-earth, and rare-earth metals. Multinary alkali polychalcogenides have been widely investigated since the development of the reactive flux method.[12−14] Examples include $A_4TM_2S_{11}$ and $A_6Nb_4Q_{22}$ (A = K, Rb; TM = Nb, Ta),[15] which contain TM_2Q_{11} units and polychalcogen units of various shapes. Alkaline-earth polychalcogenides are less common than alkali metal polychalcogenides, and known examples include $Sr_6Sb_6S_{17}$,[16] $Ba_9Nb_4S_{21}$,[17] $K_4Ba_2(Nb_2S_{11})_2$,[18] $K_2BaTa_2S_{11}$,[19] $Ba_4SiSb_2Se_{12}$,[20] and $Ba_2Sn_2Te_5$,[21] which contain coordinated oligomeric motifs. Some polyselenides contain mixed alkali and rare-earth metals, such as ATh_2Se_6 (A = K, Rb),[22] which contains a superstructure arising from ordered Se_2^{2-} and Se^{2-} units.

Based on a review of the literature, no previous report has focused on compounds in the ternary polychalcogenide system Ae−TM−Q (Ae = alkaline-earth element; TM = V, Nb, Ta). In this study, we investigated the ternary chalcogenide system in the Ae−TM−Q system by varying the relative compositions of alkaline-earth (Sr, Ba), early transition-metal (V, Nb, Ta), and group-16 elements (S, Se, Te) to establish new solid-state compounds. In our exploratory study of alkaline-earth polychalcogenides, we prepared and characterized new polychalcogenides of the form $Ba_3TM_2Se_9$ (TM = Nb or Ta), which feature a new structural type. Single-crystal and powder X-ray diffraction analyses were performed to understand the crystal structure. Measurements of diffuse reflectance and electrical resistivity were used to determine the band gap. Raman spectra were recorded, and the electronic structure was calculated for these compounds to understand the structure and bonding in the system.

EXPERIMENTS

Syntheses. All operations on chemicals and compounds were performed in a glovebox in a nitrogen atmosphere. Chemicals (Alfa

Received: June 8, 2013

   dx.doi.org/10.1021/ic4013763 | Inorg. Chem. XXXX, XXX, XXX−XXX

Aesar) were used as obtained: Sr, 99.00%, chunks; Ba, 99.00%, chunks; Nb, 99.90%, powder; Ta, 99.50%, powder; Sb, 99.90%, powder; S, 99.5%, powder; Se, 99.95%, powder; and Te 99.99%, powder. In typical reactions, the reaction mixtures in stoichiometric proportions (total mass = ~0.5 g) were placed in silica tubes, which were subsequently flame-sealed in a vacuum. These tubes were placed in a computer-controlled furnace for reaction. The elemental mixtures were heated to 1023 K within 1 day, maintained for 1 day, and slowly cooled to 673 K within 1 day. BaSe was synthesized as a precursor, which was obtained from the stoichemical mixture of the elements Ba (chunks) and Se (powder), annealed at 823 K for more than 1 week, and spontaneously cooled to room temperature.

An unknown phase was initially observed in the powder X-ray diffraction (PXRD) pattern of the reaction product Ba/Ta/Sb/Se = 4/1/1/16.2. Suitable pieces were selected for single-crystal X-ray diffraction (SXRD). The SXRD refinement confirmed the formula to be $Ba_3Ta_2Se_9$, featuring a new structural type. The elements Ba, Ta, and Se were mixed in a mmol ratio of 3:2:9, heated by using the aforementioned temperature program, and yielded a pure phase of $Ba_3Ta_2Se_9$. We also prepared analogues of $Ae_3TM_2Q_9$ with Ae = Sr, Ba; TM = Nb, Ta; Q = S, Se, Te. Characterization using PXRD, the "$Ba_3Nb_2Se_9$" reaction produced a mixture of $BaSe_2$ and unknown phases that exhibited a PXRD pattern similar to that of $Ba_3Ta_2Se_9$. The remaining reactions yielded known compounds, listed in Supporting Information Table S1. After the SXRD refinement was completed, the unknown phase was identified as $Ba_3Nb_2Se_9$, which was obtained in a pure phase of slowly heating reactive mixtures of BaSe, Nb, and Se in the molar ratio BaSe/Nb/Se = 3:2:6 to 823 K over 1 week and annealing for 1 month. After switching off the power of the furnace, the product was cooled to room temperature. The PXRD patterns of the title compounds are illustrated in Figure 1, which includes

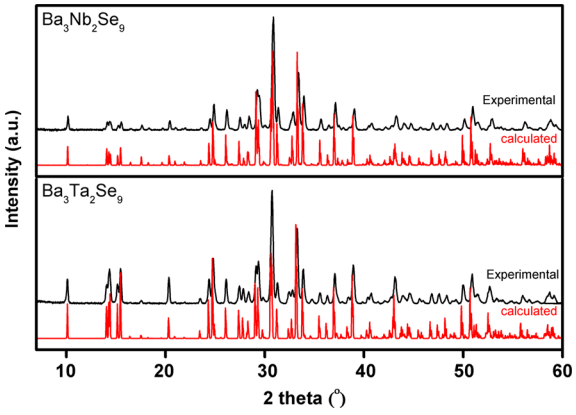

Figure 1. Experimental and calculated patterns of powder X-ray diffraction for $Ba_3Nb_2Se_9$ and $Ba_3Ta_2Se_9$.

comparisons of their calculated patterns. $Ba_3Nb_2Se_9$ is unstable in the presence of O_2 and H_2O and should be stored in a vacuum, whereas $Ba_3Ta_2Se_9$ is stable in moist air for more than 1 month.

Characterization. PXRD (Bruker D8 Advance diffractometer operated at 40 kV and 40 mA, Cu Kα radiation, λ = 1.5418 Å) data were obtained in a 2θ range from 7° to 60° by using a step size of 0.016° and an exposure interval of 0.1 s/step. Differential thermal analysis (DTA) was performed with a Netzsch STA 409PC device. Powder samples were placed into flame-sealed quartz capsules contained in Al_2O_3 crucibles. After heating to 1073 K at a rate of 10 K/min, the samples were cooled to 673 at 10 K/min under a constant flow of N_2. The diffuse reflectance was measured using a UV–visible spectrophotometer (Jasco V-570) near 298 K, and an integrating sphere was used to measure the spectra over a range of 200–2400 nm. Ground powder samples were pressed onto a thin quartz slide holder, and a $BaSO_4$ plate was used as the reference. The electric resistivity was measured following a standard four-probe method on cold-pressed bars (1 × 1 × 5 mm^3). The sample $Ba_3Ta_2Se_9$ was annealed at 673 K for 1 week before the measurement, and the resistivity data of $Ba_3Nb_2Se_9$ were directly collected on the cold-pressed bar to prevent decomposition of the compound. Five scans of the Raman spectra (Bruker RSF-100 FT-Raman spectrometer equipped with a Nd/YAG laser, λ = 1064 nm) on the powder samples placed in silica tubes (i.d. = 3 mm) were performed to cover a range of 200–400 cm^{-1}.

Crystallographic Measurements. Single crystals of $Ba_3Nb_2Se_9$ and $Ba_3Ta_2Se_9$ were obtained on crushing polycrystalline samples. Suitable crystals with a metallic luster were mounted on glass fibers with epoxy resin glue for SXRD measurement. The intensity data were collected (Bruker X8 APEX diffractometer using graphite-monochromatic Mo–Kα radiation, λ = 0.71073 Å) at 273 K, and the distance between the sample crystal and the detector was 4.0 cm. The 2θ values cover the range from 4.04° and 50.22°. The diffraction intensities of all frame data were used to determine the parameters of the unit cell. The program package[23] APEX 2 was used to determine and refine the structure. Multiscan absorption corrections were applied using the SADABS program. The structure solution provided two possible models with space groups $P2_1/c$ (14) and $C2/c$ (15), on which the refinement in the space group $C2/c$ provided a smaller R value than did that with the space group $P2_1/c$. To verify this conclusion, a recombination of the zone images of $Ba_3Nb_2Se_9$ and $Ba_3Ta_2Se_9$ are respectively illustrated in Supporting Information Figures S1a and S1b. The diffraction signals resulting from the $(h0l)$ ($h = 2n+1$, $l = 2n'$) planes were present but weak in both cases, and corresponded to the systematic absence of space group $P2_1/c$. The direct method provided 14 unique sites: five metal and nine Se sites. The determinations of the coordination and electronic density revealed that three Ba sites, two TM (TM = Nb or Ta) sites, and nine Se sites could be satisfactorily refined using reasonable isotropic displacement parameters. After refinement of the anisotropic displacement parameters for all atoms, the R-value was approximately 0.02 and the residual electron density was less than 2 e $Å^{-3}$. The SXRD refinement results are listed in Table 1 and Supporting Information Table S2.

Table 1. Crystal Data and Structure Refinement for Compounds $Ba_3TM_2Se_9$ (TM = Nb, Ta)

refined composition	$Ba_3Nb_2Se_9$	$Ba_3Ta_2Se_9$
temperature (K)	273(2)	273(2)
wavelength (Å)	0.71073	0.71073
crystal system	monoclinic	monoclinic
space group, Z	$P\ 2_1/c$ (14),2	$P\ 2_1/c$ (14), 2
a (Å)	7.359(2)	7.3579(8)
b (Å)	12.383(3)	12.374(1)
c (Å)	17.574(4)	17.593(2)
β (deg)	97.147(5)	97.359(2)
V ($Å^3$)	1589.0(7)	1588.6(3)
θ_{min}, θ_{max} (deg)	2.02 to 25.03	2.02 to 25.11
independent reflns (R_{int})	2807 (0.0376)	2825 (0.0386)
obsd reflns	13794	13765
d_{calcd} (mg m^{-3})	5.47	6.207
abs coeff (mm^{-1})	29.302	41.631
GOF on iF^2	0.984	1.026
R1, wR2 ($I > 2\sigma(I)$)	0.0278, 0.0565	0.0319, 0.0837
R1, wR2 (all data)[a]	0.0455, 0.0620	0.0398, 0.0882
largest diff. peak and hole (e $Å^{-3}$)	1.238, −1.051	1.609, −2.483

[a] $R1 = \Sigma||F_0 - F_c||/\Sigma|F_0|$. $wR2 = \{\Sigma[w(F_0^2 - F_c^2)^2]/\Sigma[w(F_0^2)^2]\}^{1/2}$.

Calculation of Electronic Structure. Tight binding of the linear muffin-tin orbitals (LMTO) with an atomic-sphere approximation (ASA) was used to evaluate the electronic structure. In LMTO, we applied the density-functional theory with local-density approximation (LDA).[24–27] The electronic structure of $Ba_3Ta_2Se_9$ was calculated using the SXRD data. A k-space integration was performed on a grid of more than 300 independent k-points. We analyzed the electronic

dx.doi.org/10.1021/ic4013763 | Inorg. Chem. XXXX, XXX, XXX–XXX

structure using information from densities of states (DOS), band structure,[28] and crystal orbital Hamiltonian population (COHP) curves.[29]

RESULTS AND DISCUSSION

Structure Description. $Ba_3TM_2Se_9$ (TM = Nb, Ta) crystallize in a new structure type in the monoclinic space

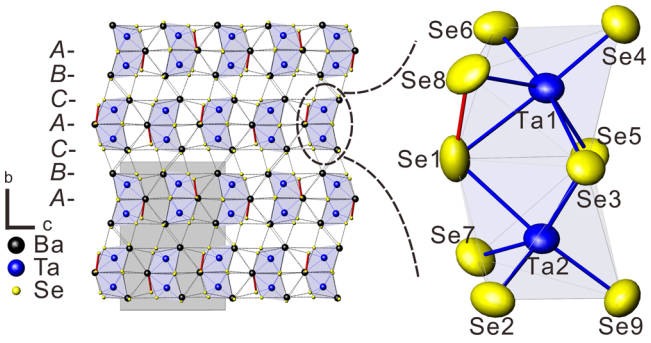

Figure 2. Perspective view of $Ba_3Ta_2Se_9$ structure along the *a*-axis with its ellipsoid plot of the $Ta_2Se_9^{-6}$ unit. The red bonds indicate the short Se−Se contacts.

group $P2_1/c$ (14). The compounds comprised 14 independent crystallographic sites: three sites for Ba, two sites for TM (TM = Nb, Ta), and nine sites for Se. Figure 2 displays a perspective view of the structure of $Ba_3Ta_2Se_9$ along the *b*-axis to facilitate discussion on its structure. The structure may be described as a distorted hexagonal close-packed (HCP) structure comprising Ba and Se atoms in a Ba:Se ratio of 1:3. The HCP layers are arranged in an *ABCACB* sequence, and within these layers, the Ta atoms fill one-sixth of the octahedral holes to form distorted $TaSe_6$ octahedra. These units share a face to form a $[Ta_2Se_9]^{6-}$ unit, which contains a Se_2^{2-} diselenide fragment (Figure 2). The $TaSe_6$ octahedra are characterized by four short (2.39−2.55 Å) and two long (2.74−2.94 Å) Ta−Se contacts with Se−Ta−Se angles from 78° to 104°, and is comparable with the Ta−Se contacts and the Se−Ta−Se angles in $TlTaSe_3$.[30] The bioctahedral Ta_2Se_9 unit contains one short homonuclear Se−Se contact with a length of 2.50 Å. Compared with the longer Se···Se distance in a range 2.95−3.92 Å in $Ba_3Ta_2Se_9$, the short Se−Se distance indicates the formation of a Se_2^{2-} unit. Similar Se_2^{2-} units were reported for $Sr_4Sn_2Se_9$[31] (d_{Se-Se} = 2.46 Å). The Ta atoms are in a distorted octahedral coordination environment caused by the short Se−Se contact and interactions between Se_2^{2-} and Ta. The Ta_2Se_9 unit carries a charge of −6, which is balanced by three Ba^{2+} cations. The Ba−Se contacts were in the range of 3.30 to 4.37 Å, with a coordination number of 11 or 12. The charge-balanced formula could therefore be written as $(Ba^{2+})_3$ $(Ta^{5+})_2$ $(Se^{2-})_7$ (Se_2^{2-}).

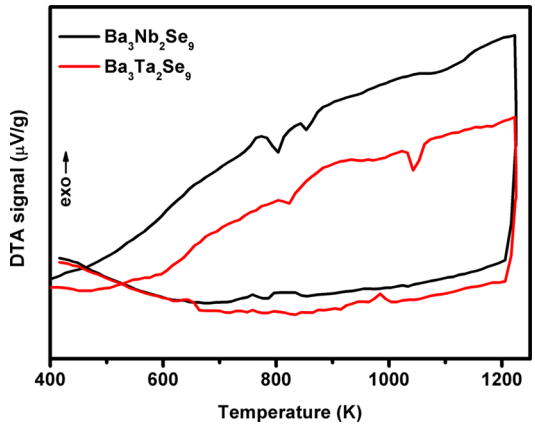

Figure 4. DTA curves for $Ba_3Nb_2Se_9$ (black) and $Ba_3Ta_2Se_9$ (red).

The crystal structure of $Ba_3TM_2Se_9$ (TM = Nb, Ta) was compared to related compounds, namely, $Sr_{0.9}La_{0.1}MnO_3$,[32] $BaNb_{0.8}Se_3$,[33] and $Cs_3Ho_2Br_9$[34] in Figure 3. These compounds contain close-packed layers of atoms with varied sequences and occupied sites for incorporated atoms. For $PuAl_3$,[35] 6H-SiC,[36] and $Sr_{0.9}La_{0.1}MnO_3$,[32] the crystal structures of these phases contain the same HCP sequence as the title compound. Taking $Sr_{0.9}La_{0.1}MnO_3$[32] (Figure 3a) as an example, the atomic ratio of metal (0.9 Sr^{2+} + 0.1 La^{3+}) to oxygen atoms in the HCP layers is 1:3. Of the interstitial octahedral sites, a quarter is occupied with Mn atoms. The crystal structure of $BaNb_{0.8}Se_3$[33] (Figure 3b) indicates that the close-packing sequence is ABAB for $^3_\infty[BaSe_3]^{-4}$ and the Nb atoms partially fill the octahedral holes (80%). The structure contains 1D chains of face-shared $^1_\infty[NbSe_3]^{-2}$ units (Figure 3b). The last example $Cs_3Ho_2Br_9$[34] exhibits the same elemental ratio as $Ba_3TM_2Se_9$ (TM = Nb, Ta), but the crystal structure contained a packing sequence ABAB for $^3_\infty[CsBr_3]^{2-}$ and the arrangement of the edge-shared units $[Ho_2Br_9]^{3-}$ differed from that of $Ba_3TM_2Se_9$ (Figure 3c).

Physical Properties. We applied DTA to investigate thermal stability, and the curves are illustrated in Figure 4. Overall, for both compounds two endothermic signals are observed that correspond to the melting and decomposition, which began respectively at 788 and 845 K for $Ba_3Nb_2Se_9$ and 810 and 1032 K for $Ba_3Ta_2Se_9$. To understand the decomposition, we heated the as-prepared samples to the selected temperatures, and subsequently quenched them in a water bath. PXRD was conducted, and the results are displayed in Supporting Information Figures S2 and S3. $Ba_3Nb_2Se_9$ was identified after quenching at 823 K, whereas the product of the quenching reaction at 998 K contained mixtures of $BaNb_{0.8}Se_3$ and $BaSe_2$ (Supporting Information Figure S2). Similar results

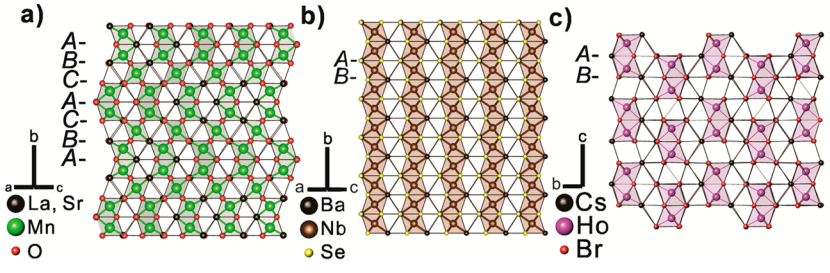

Figure 3. Related structures of $Sr_{0.9}La_{0.1}MnO_3$ (a), $BaNb_{0.8}Se_3$ (b), and $Cs_3Ho_2Br_9$ (c).

dx.doi.org/10.1021/ic4013763 | Inorg. Chem. XXXX, XXX, XXX−XXX

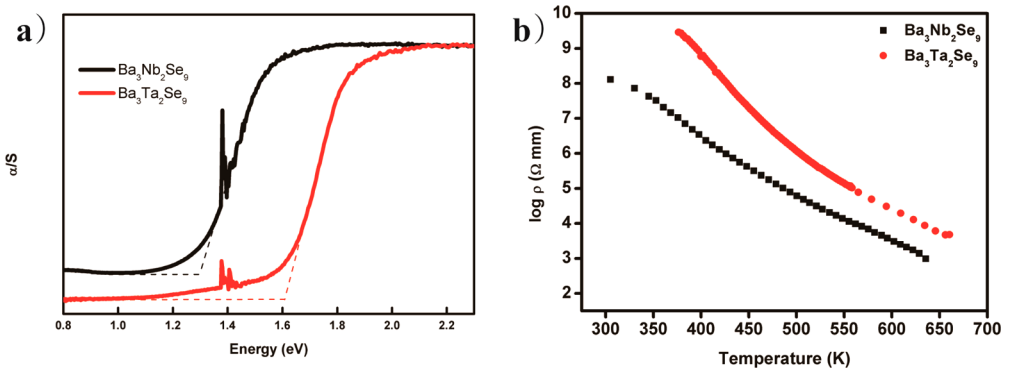

Figure 5. UV−vis reflectance spectra and temperature dependence of electronic resistivity of $Ba_3Nb_2Se_9$ (black) and $Ba_3Ta_2Se_9$ (red).

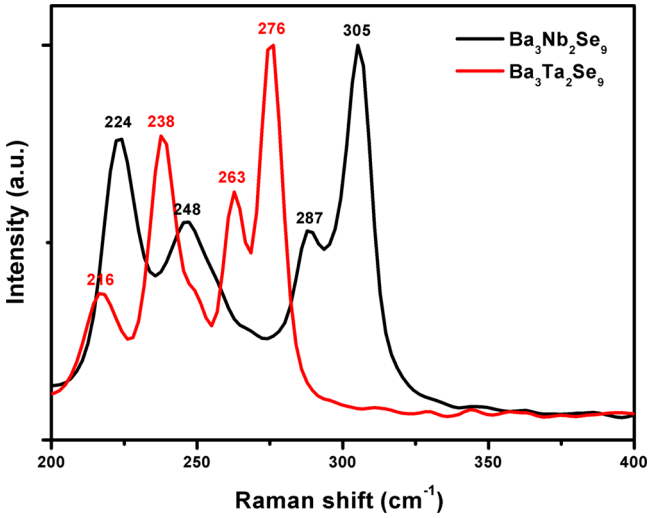

Figure 6. Raman spectra of $Ba_3Nb_2Se_9$ (black) and $Ba_3Ta_2Se_9$ (red).

were discovered in the $Ba_3Ta_2Se_9$ (Supporting Information Figure S3) sample, supporting our hypothesis.

We determined the optical band gaps for $Ba_3TM_2Se_9$ (TM = Nb, Ta) according to UV−vis diffuse-reflectance spectra, as indicated in Figure 5a. The spectra demonstrated abrupt absorptions and the measured optical band gaps were 1.3 eV for $Ba_3Nb_2Se_9$ and 1.6 eV for $Ba_3Ta_2Se_9$. The sharp peaks at 1.38 eV (λ = 900 nm) originated from the changes of the detectors and grating. The electronic resistivity was measured, and the plots of the temperature dependence of resistivity indicated that the resistivity shows a decrease as the temperatures increases, indicating semiconducting behavior (Figure 5b). The activation energies for both compounds were evaluated using the Arrhenius' equation, and the results were 0.69 eV for $Ba_3Nb_2Se_9$ and 1.05 eV for $Ba_3Ta_2Se_9$, as shown in Supporting Information Figure S4. This trend is consistent with the measured optical band gaps.

The Raman spectrum of the title compounds in Figure 6 shows four distinct lines at 216, 238, 263, and 276 cm^{-1} for $Ba_3Nb_2Se_9$, and at 224, 248, 287, and 305 cm^{-1} for $Ba_3Ta_2Se_9$. In both compounds, shifts in the range of 210−250 cm^{-1} were assigned as Se_2^{2-} stretching vibrations. According to the published spectra of various polyselenides, the Se_2^{2-} stretching vibrations are in the range of 215−266 cm^{-1} depending on the coordination environment of the Se atom and metal atoms bonded to Se. For example, $Rb_2BaNb_2Se_{11}$[37] and $Tl_4Ta_2Se_{11}$[38] sharing similar building units, $[TM_2Se_{11}]^{4-}$ (TM = Nb, Ta), but their Raman shifts appeared at 235 and 266 cm^{-1} for $Rb_2BaNb_2Se_{11}$, and at 215, 236, 247 cm^{-1} for $Tl_4Ta_2Se_{11}$. The remaining shifts in the 250−350 cm^{-1} range were assigned as vibrations of TM−Se (TM = Nb, Ta) contacts, and are comparable to the Raman spectra of the reported compounds.[37]

Calculations of Electronic Structure. We calculated the electronic structure of $Ba_3Ta_2Se_9$ to evaluate its properties and bonding characteristics. The total and partial DOS diagrams are

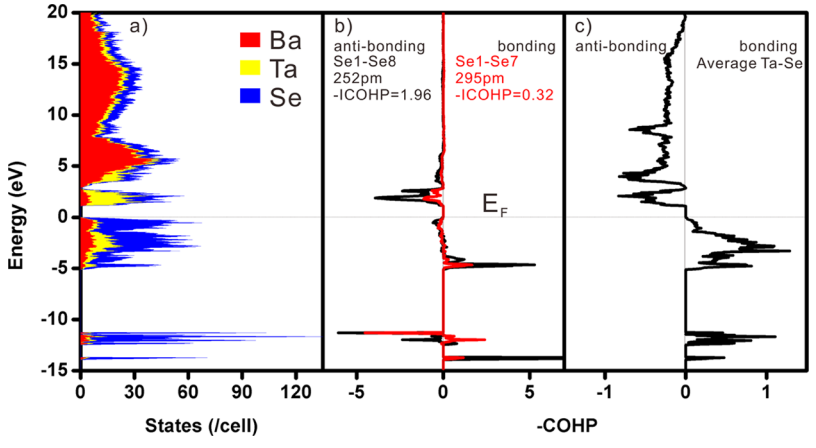

Figure 7. Total and partial densities of states for $Ba_3Ta_2Se_9$ (a): crystal orbital-Hamiltonian population curves for selected Se−Se (b) and for average Ta−Se contact (c).

dx.doi.org/10.1021/ic4013763 | Inorg. Chem. XXXX, XXX, XXX−XXX

plotted in Figure 7, and the corresponding band structure is indicated in Supporting Information Figure S5. According to the band structure, the title compound exhibits a direct band gap ~1.2 eV, which is also seen in the DOS curve. The ns states and np states of all the elements contributed to the valence band between −10 to −15 and 0 to −5 eV. Ta 5d, Ba 6s, and Ba 4f states dominated the conduction-band states in the ranges of 1−3, 3−10, and 10−20 eV, and minor mixing of Ta 6s and Se 4p states occurred.

The COHP curves for the selected Se−Se and average Ta−Se contacts are plotted in Figures 7b and 7c, respectively. The interatomic interactions of the Ta−Se contacts indicated that the bonding interactions were optimized at the Fermi level, but the Se−Se contacts exhibited antibonding characteristics near the Fermi level, which resulted from the hybridization of Se 4s and 4p states. The interactions of the Se−Se contacts with Se1−Se8 contained a large -ICOHP value 1.96 eV/bond compared with the other Se−Se contacts of which -ICOHP = ~0.32 (eV/bond), which is indicative of strong bonding between Se1−Se8.

CONCLUSION

We report the preparation and characterization of a new polyselenide $Ba_3TM_2Se_9$ (TM = Nb, Ta) that crystallizes in an unprecedented structure. A new moiety $[TM_2Se_9]^{6-}$ that contains a coordinated diselenide group Se_2^{2-} was discovered. The semiconducting property of the as-synthesized compounds was confirmed according to measurements of diffuse reflectance spectra and electrical conductivity, as well as calculations of the electronic structure. The Raman spectra and the calculated electronic structure supported the bonding characteristics of the Se−Se contacts in these compounds.

ASSOCIATED CONTENT

Supporting Information

(1) X-ray crystallographic files in CIF format, (2) the reconstructed [h0l] zone axis image of $Ba_3Nb_2Se_9$ and $Ba_3Ta_2Se_9$, (3) variation of PXRD pattern with quenching temperature for $Ba_3Nb_2Se_9$, (4) variation of PXRD pattern with quenching temperature for $Ba_3Nb_2Se_9$, (5) the Arrhenius plots for $Ba_3Nb_2Se_9$ and $Ba_3Ta_2Se_9$, (6) band structure in energy window 2 eV of $Ba_3Ta_2Se_9$, (7) summary of reactions and products of $Ae_3TM_2Q_9$ (Ae = Sr, Ba; TM = Nb, Ta; Q = S, Se, Te), (8) fractional atomic coordinates and equivalent isotropic atomic displacement parameters of $Ba_3TM_2Se_9$ (TM = Nb, Ta), and (9) select bond lengths for $Ba_3TM_2Se_9$ (TM = Nb, Ta). These materials are available free of charge via Internet at http://pubs.acs.org.

AUTHOR INFORMATION

Corresponding Author

*E-mail: chishen@mail.nctu.edu.tw.

Notes

The authors declare no competing financial interest.

ACKNOWLEDGMENTS

We thank Professor W.-G. Diau for assistance with UV diffuse reflectance measurements and Dr. R.-J. Wu of the Industrial Technology Research Institute of Taiwan for the use of FT-Raman spectrum facilities. The National Science Council, Taiwan supported this research under grant number 101-2113-M-009-017-MY3.

REFERENCES

(1) Lowhorn, N. D.; Tritt, T. M.; Abbott, E. E.; Kolis, J. W. *Appl. Phys. Lett.* **2006**, *88*, 022101/1.
(2) Shafaei-Fallah, M.; He, J.; Rothenberger, A.; Kanatzidis, M. G. *J. Am. Chem. Soc.* **2011**, *133*, 1200.
(3) Boettcher, P.; Getzschmann, J.; Keller, R. *Z. Anorg. Allg. Chem.* **1993**, *619*, 476.
(4) Boettcher, P. *Z. Anorg. Allg. Chem.* **1980**, *461*, 13.
(5) Boettcher, P. *Z. Kristallogr.* **1979**, *150*, 65.
(6) Durichen, P.; Bolte, M.; Bensch, W. *J. Solid State Chem.* **1998**, *140*, 97.
(7) Assoud, A.; Xu, J.; Kleinke, H. *Inorg. Chem.* **2007**, *46*, 9906.
(8) Bugaris, D. E.; Copping, R.; Tyliszczak, T.; Shuh, D. K.; Ibers, J. A. *Inorg. Chem.* **2010**, *49*, 2568.
(9) Kromm, A.; Sheldrick, W. S. *Z. Anorg. Allg. Chem.* **2006**, *632*, 191.
(10) Patschke, R.; Heising, J.; Schindler, J.; Kannewurf, C. R.; Kanatzidis, M. *J. Solid State Chem.* **1998**, *135*, 111.
(11) Sheldrick, W. S.; Wachhold, M. *Angew. Chem., Int. Ed. Engl.* **1995**, *34*, 450.
(12) Sunshine, S. A.; Kang, D.; Ibers, J. A. *J. Am. Chem. Soc.* **1987**, *109*, 6202.
(13) Kanatzidis, M. G. *Chem. Mater.* **1990**, *2*, 353.
(14) Kanatzidis, M. G.; Sutorik, A. C. *Prog. Inorg. Chem.* **1995**, *43*, 151.
(15) Bensch, W.; Durichen, P.; Nather, C. *Solid State Sci.* **1999**, *1*, 85.
(16) Choi, K.-S.; Kanatzidis, M. G. *Inorg. Chem.* **2000**, *39*, 5655.
(17) Saeki, M.; Onoda, M. *Bull. Chem. Soc. Jpn.* **1991**, *64*, 2923.
(18) Wu, Y.; Naether, C.; Lehnert, N.; Bensch, W. *Solid State Sci.* **2005**, *7*, 1062.
(19) Wu, Y.; Bensch, W. *Z. Naturforsch., B: J. Chem. Sci.* **2010**, *65*, 1219.
(20) Choi, K.-S.; Kanatzidis, M. G. *Inorg. Chem.* **2001**, *40*, 101.
(21) Assoud, A.; Derakhshan, S.; Soheilnia, N.; Kleinke, H. *Chem. Mater.* **2004**, *16*, 4193.
(22) Choi, K.-S.; Patschke, R.; Billinge, S. J. L.; Waner, M. J.; Dantus, M.; Kanatzidis, M. G. *J. Am. Chem. Soc.* **1998**, *120*, 10706.
(23) Bruker; 2.1 ed.; Bruker AXS Inc.: Madison, WI, 2006.
(24) van Barth, U.; Hedin, L. *J. Phys. C* **1971**, *4*, 2064.
(25) Andersen, O. K. *Phys. Rev. B* **1975**, *12*, 3060.
(26) Skriver, H. L. *The LMTO Method*; Springer: Berlin, 1984.
(27) Blöhl, P. E.; Jepsen, O.; Andersen, O. K. *Phys. Rev. B: Condens. Matter* **1994**, *49*, 16223.
(28) Jepsen, O.; Andersen, O. K. *Z. Phys.* **1995**, *97*, 25.
(29) Dronskowski, R.; Blöhl, P. E. *J. Phys. Chem.* **1993**, *97*, 8617.
(30) Teske, C. L.; Bensch, W.; Benea, D.; Minar, J.; Perlov, A.; Ebert, H. *Z. Naturforsch., B: Chem. Sci.* **2005**, *60*, 858.
(31) Pocha, R.; Johrendt, D. *Inorg. Chem.* **2004**, *43*, 6830.
(32) Mori, T.; Kamegashira, N. *J. Alloys Compd.* **2000**, *313*, L1.
(33) Ohtani, T.; Honji, S.; Takano, M. *J. Solid State Chem.* **1997**, *132*, 188.
(34) Doenni, A.; Fischer, P.; Furrer, A.; Cockcroft, J. K.; Guedel, H. U. *J. Solid State Chem.* **1991**, *93*, 119.
(35) Larson, A. C.; Cromer, D. T.; Stambaugh, C. K. *Acta Crystallogr.* **1957**, *10*, 443.
(36) Bind, J. M. *Mater. Res. Bull.* **1978**, *13*, 91.
(37) Wu, Y.; Naether, C.; Bensch, W. *J. Solid State Chem.* **2007**, *180*, 113.
(38) Teske, C. L.; Lehnert, N.; Bensch, W. *Z. Anorg. Allg. Chem.* **2002**, *628*, 2651.

dx.doi.org/10.1021/ic4013763 | *Inorg. Chem.* XXXX, XXX, XXX−XXX